

# Functionalization of Graphene Oxide Layers Simultaneously with Liquid Phase Exfoliation

L. Anjo<sup>1</sup>, A. Arshakyan<sup>1</sup>, N. Gasparyan<sup>1</sup>, A. Shahinyan<sup>1</sup>, E. Aleksanyan<sup>2</sup>, N. Margaryan<sup>1</sup>

<sup>1</sup>*Experimental Physics Division, A. Alikhanyan National Science Laboratory (Yerevan Physics Institute),  
2 Alikhanyan Brothers, Yerevan, Armenia*

<sup>2</sup>*Applied Physics Research Division, A. Alikhanyan National Science Laboratory (Yerevan Physics Institute),  
2 Alikhanyan Brothers, Yerevan, Armenia*

Email: n.margaryan@erphi.am

(Received: May 20, 2023; Revised: June 5, 2023; Accepted: June 10, 2023)

**Abstract.** Graphene oxide (GO) has garnered significant interest for its exceptional properties and potential applications in various fields. This study investigated the disparities between graphene oxide synthesized in an ammonia-acetone solution and graphene oxide synthesized in acetone using the exfoliation method. Raman spectroscopy, FTIR spectroscopy, and current-voltage characteristics analysis were employed to evaluate the samples. Raman spectroscopy analysis revealed distinct differences in the molecular composition and structural characteristics of the samples, as indicated by variations in the "D," "G," and "2D" peaks. FTIR spectroscopy identified various functional groups in both samples, with changes attributed to the presence of ammonium in one sample. Furthermore, the current-voltage characteristics analysis was conducted to assess the electrical properties of the graphene films. Results of the current-voltage characteristics analysis showed that the conductivity of the membranes obtained in an acetone medium was approximately an order of magnitude higher than that of the membranes obtained in an ammonia medium. This discrepancy suggests that the exfoliation in an acetone medium resulted in stronger doping of the graphene layers compared to the exfoliation in an ammonia solution. The linearity observed in the current-voltage characteristics can be attributed to the presence of a significant number of free electrons in the conduction band of the samples due to doping. These findings provide valuable insights into the structural, compositional, and electrical properties of graphene oxide synthesized using different methods and precursor solutions. Understanding these disparities is crucial for tailoring graphene-based materials to specific applications.

**Keywords:** graphene oxide, FTIR, Raman, I-V characteristics

DOI:10.54503/18291171-2023.16.2-56

## 1. Introduction

Graphene, a two-dimensional material with extraordinary electronic, mechanical, and optical properties, has attracted considerable engagement in recent years due to its conceivable applications in various fields such as electronics, energy storage, and biomedical engineering [1–5]. Graphene is a single layer of carbon atoms organized in a hexagonal lattice structure. Its high surface area and excellent electrical conductivity make it an immaculate material for electrochemical applications. Graphene oxide (GO) is a derivative of graphene, which is produced by oxidizing graphene. GO has many oxygen-containing functional groups such as hydroxyl, epoxy, and carboxyl, which make it a versatile material for various applications [6–9]. GO can be effortlessly functionalized with different molecules and can be utilized as a precursor for the synthesis of other graphene-based materials. Graphene Oxide can also be used for the synthesis of graphene-based nanocomposites. Graphene-based nanocomposites have attracted substantial attention due to their excellent mechanical, thermal, and electrical properties [10–13]. Graphene oxide can be functionalized with different molecules to improve its dispersibility in various solvents and to enhance its compatibility with different matrices. One of the most reasonable methods of synthesis that recently attracted attention is the Exfoliation method. Exfoliation has many advantages over other methods of graphene synthesis that are important are: cost-effectiveness and high productivity: Exfoliation

methods are moderately low cost and can yield a high quantity of graphene sheets. This is exceptionally true for liquid-phase exfoliation techniques such as sonication, which can produce considerable quantities of graphene quickly [14–16].

**Fewer defects:** Exfoliation methods can produce high-quality graphene sheets with fewer defects compared to other synthesis methods. This is because exfoliation methods do not require high temperatures or harsh chemicals, which can introduce defects into the graphene lattice [17–18].

**Tailored properties:** Exfoliation methods allow to produce graphene with tailored properties. Adjusting the processing conditions makes producing graphene sheets with specific sizes, shapes, and functionalization possible, which can be useful for different applications [19–20].

**Scalability:** Exfoliation methods are effortlessly scalable and can be acclimated for large-scale production. This is especially crucial for industrial applications, where large quantities of graphene are required [21–23].

Graphene-centered nanocomposites have also been synthesized using ammonia and acetone as precursors. Ammonia and acetone are easily available and affordable precursors for the synthesis of graphene-centered nanocomposites [24–27]. Graphene-centered nanocomposites synthesized using ammonia and acetone have shown extraordinary electrochemical properties and have been utilized as electrode materials in supercapacitors. This research focuses on the disparities between graphene oxide synthesized in an ammonia-acetone solution and graphene oxide synthesized in acetone utilizing the exfoliation method. We investigate the samples using FTIR, Raman spectroscopy, and current-voltage characteristics.

## 2. Materials and Methods

The materials used in this experiment included graphene powder (Alfa Aesar, Stock #14736, Lot #H14N11) with particle sizes of approximately 20-25 nanometers, 30 ml of 99.6% acetone, and 30 ml of 25% ammonia.

Graphite powder was solved in acetone and ammonia solutions. Next, the acetone and ammonia solutions were each placed separately in the ultrasonic device for 15 minutes with a power of 50 watts. The ultrasonic waves promote exfoliation by causing twisting deformation between graphite layers. Exfoliated graphene flakes formed integral layers by grouping on the surface of the solutions. The layers were directly removed from the surfaces of the solutions and deposited on 600  $\mu$  NaCl substrates. Agilent Cary 630 spectrometer and Horiba Explora microscope were used for FTIR and Raman measurements. The I-V characteristics were measured in LabVIEW medium using National Instruments data acquisition (DAQ) device.

## 3. Investigation and Analysis

### 3.1. Raman spectroscopy

Raman spectroscopy is one of the best methods to characterize graphene and related materials. Raman spectra are the fingerprints of these nanomaterials.

In this study, two Raman spectroscopy analyses were conducted to investigate the properties of the samples. sample 1 revealed a prominent "D" peak at 1345  $\text{cm}^{-1}$ , indicating specific vibrational modes associated with the molecular structure of acetone and graphene. In sample 2, the "D" peak showed a shift towards 1330  $\text{cm}^{-1}$  with reduced intensity, suggesting variations in the molecular composition or structural characteristics of ammonia and graphene. These findings highlight distinct spectral features between the two analyses, potentially reflecting differences in the chemical properties and structural changes of the investigated samples. Furthermore, the "G" peak in the Raman spectrum is a characteristic feature of graphene and provides important information

about its structural properties. It arises from the in-plane vibrational motion of carbon atoms in the  $sp^2$  hybridized lattice structure of graphene. The position and shape of the "G" peak are influenced by various factors, including the number of graphene layers, defects, strain, and doping. In Figure 1a, the "G" peak is observed at a wavelength of  $1577\text{ cm}^{-1}$  in the Raman spectrum, indicating the presence of graphene in the sample. The position of the "G" peak remains relatively unchanged between the two samples, suggesting similar lattice structures. In Figure 1b, the "G" peak is observed at a slightly lower wavelength of  $1565\text{ cm}^{-1}$ . This shift can be attributed to different strain levels or doping effects in the graphene sample. Additionally, the intensity of the "G" peak in sample 2 is reduced compared to sample 1, which may indicate differences in the quality or degree of disorder in the graphene lattice. Due "2D" peak is observed at around 400 intensity in sample 1, while in sample 2, it is observed at approximately 250 intensity. The intensity difference of the "2D" peak between the two analyses suggests variations in the number of layers or structural features of the graphene samples. These differences indicate the presence of multilayer graphene in sample 1 analysis and monolayer graphene in the other. Additionally, these variations could also signify changes in the quality or structural characteristics of the graphene samples [1, 29].

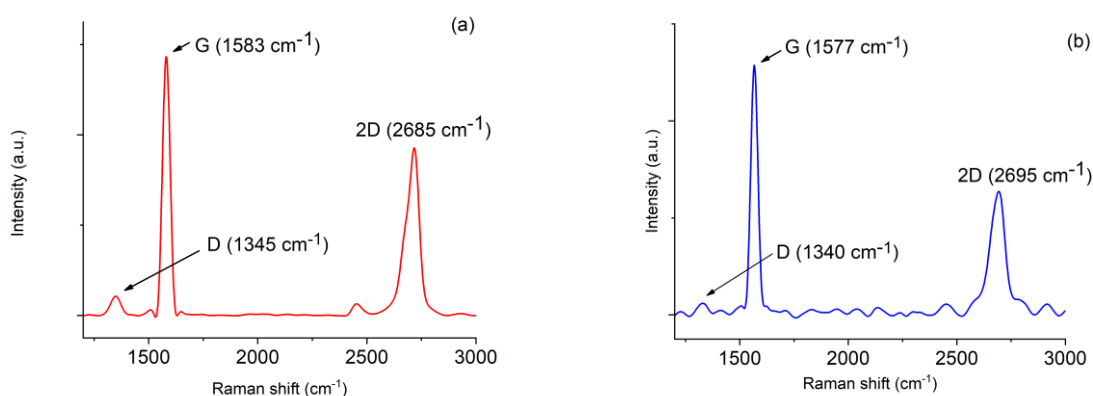


**Fig. 1:** Raman spectroscopy of graphene layers exfoliated in acetone (a) and ammonia (b).

### 3.2. FTIR spectroscopy

FTIR spectrum of the sample ( $4000\text{--}400\text{ cm}^{-1}$ ) showed prominent peaks indicating various functional groups. In the  $3000\text{--}3350\text{ cm}^{-1}$  region, amid or NH bonds are observed. In the  $1500\text{--}1600\text{ cm}^{-1}$  region, carbonyl or CO bonds are observed, and finally, in the  $1000\text{--}1200\text{ cm}^{-1}$  region,  $sp^3$  carbon-oxygen or C-O bonds are observed. In Fig. 2(a) The peaks at  $871\text{ cm}^{-1}$ ,  $1642\text{ cm}^{-1}$ ,  $2856\text{ cm}^{-1}$  and  $2924\text{ cm}^{-1}$ ,  $3340\text{ cm}^{-1}$  in Gr corresponded to C-H bending vibrations, C=C stretching, C-H stretching, and O-H stretching, respectively. The peak below  $1077\text{ cm}^{-1}$  can be assigned to a primary alcohol. [29–33]. In Fig. 2(b) N-Gr, the significant peaks at  $870\text{ cm}^{-1}$ ,  $1175\text{ cm}^{-1}$  and  $1303\text{ cm}^{-1}$ ,  $1397\text{ cm}^{-1}$ , and  $1721\text{ cm}^{-1}$  indicate C-H bending, C-N stretching, COOH, and C=O stretching vibrations [29, 33–34]. FTIR spectroscopy suggests a complex mixture of organic compounds including epoxy groups, amines, nitriles, carboxylic acids, and carbonyl/carboxyl groups in the sample. Based on the intensity of the bands, it can be concluded that the sample contains amid, carbonyl, and  $sp^3$  carbon-oxygen bonds. Furthermore, by comparing this spectrum with a similar spectrum of pure graphene, it can be concluded that the presence of ammonium has caused a change in the electronegativity of the carbon graphene atoms.

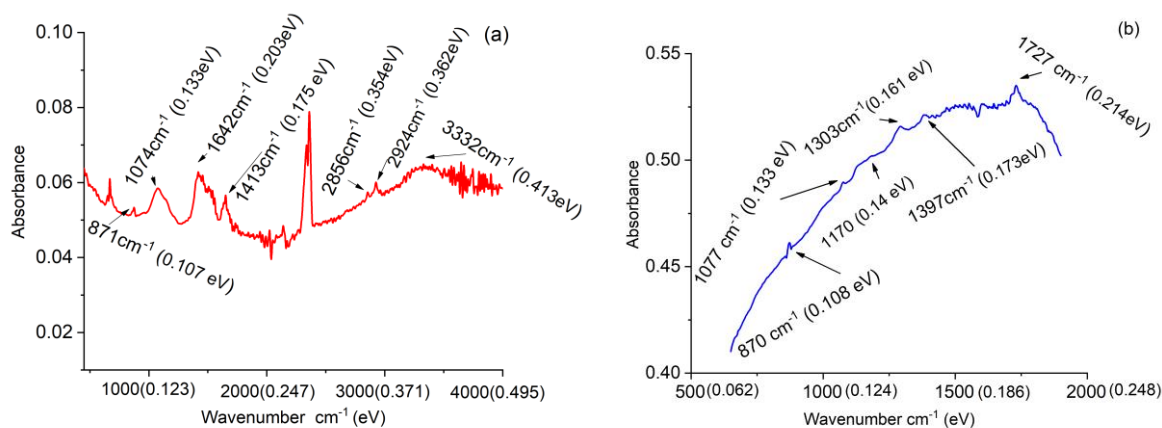


**Fig. 2:** FTIR acetone and graphene (a), ammonia and graphene (b).

### 3.3. Current-voltage characteristics

One of the important physical features of graphene is the current-voltage characteristic [35–36]. A National Instruments MyDAQ data measurement device and LabVIEW software were used to measure the current-voltage characteristics of the samples. Ohmic contacts are formed by silver deposition. Figure 3 shows the results of samples obtained by liquid-phase exfoliation method. Figure 3 (a) shows the current-voltage characteristic of two graphene films obtained in an acetone medium, and (b) of two films exfoliated in an aqueous ammonia solution. Comparative analysis of these results shows that the conductivity of films obtained in an acetone medium is an order of magnitude higher than the conductivity of a film obtained in an ammonia. Moreover, sheet resistance of the samples exfoliated in acetone and ammonia solutions are measured by four probe method. The sheet resistance of the samples exfoliated in acetone solution was about  $10\text{ M}\Omega$  which is higher than the sheet resistance of the sample exfoliated in ammonia solution ( $2\text{ M}\Omega$ ). This suggests that, as a result of exfoliation in an acetone medium, the graphene layers were doped more strongly than in the case of the ammonia solution. The linearity of the resulting current-voltage characteristics is also due to the doping factor.

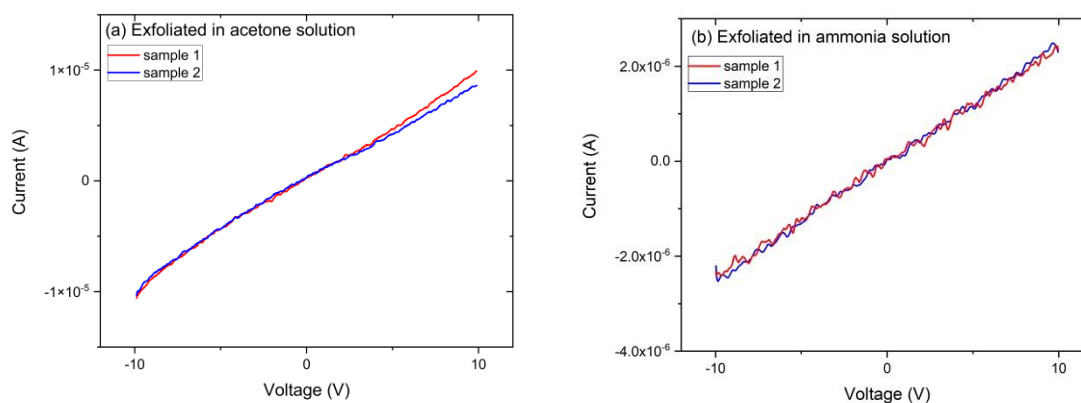


**Fig. 3:** Current-voltage characteristics of graphene layers exfoliated in acetone (a) and ammonia (b).

## 4. Conclusion

This study investigated the properties of graphene oxide synthesized in an ammonia-acetone solution and graphene oxide synthesized in acetone using the exfoliation method. Raman spectroscopy and FTIR spectroscopy were employed to analyze the samples. The results revealed distinct differences between the two samples. Raman spectroscopy analysis showed variations in the "D" and "G" peaks between the samples, indicating differences in the molecular composition and structural characteristics. The intensity and position of the "2D" peak also differed, suggesting variations in the number of graphene layers and structural features. These differences indicated the presence of multilayer graphene in one sample and monolayer graphene in the other. FTIR spectroscopy identified various functional groups in both samples, including amide, carbonyl, and sp<sup>3</sup> carbon-oxygen bonds. The presence of ammonium in one sample caused a change in the electronegativity of the graphene carbon atoms. The conductivity of the graphene films obtained in acetone was found to be significantly higher than those obtained in an ammonia solution, indicating stronger doping in the acetone medium. The findings highlight the importance of synthesis methods and precursor solutions in determining graphene oxide's structural, compositional, and electrical properties. Understanding these disparities can contribute to the development of tailored graphene-based materials for various applications.

## Acknowledgment

The work was supported by the Science Committee of RA, in the frame of the research project 21DP-1C014.

## References

- [1] N. Margaryan, N. Kokanyan, E. Kokanyan, *Journal of Saudi Chemical Society* **23** (2019) 13.
- [2] A.K. Geim, K.S. Novoselov, *Nature Materials* **6** (2007) 183.
- [3] K.S. Novoselov, A.K. Geim, S.V. Morozov, D. Jiang, Y. Zhang, S.V. Dubonos, I.V. Grogorieva, A.A. Firsov, *Science* **306** (2004) 666.
- [4] E. Ghavidel, A.H. Sari, D. Dorranean, *Optics & Laser Technology* **103** (2018) 155.
- [5] K.S. Novoselov, V.I. Fal'ko, L. Colombo, P.R. Gellert, M.G. Schwab, K. Kim, *Nature* **490** (2012) 192.
- [6] L.A. Chernozatonskii, Yu.V. Gulyaev, Z.Ja. Kosakovskaja, N.I. Sinitsyn, G.V. Torgashov, Yu.F. Zakharchenko, E.A. Fedorov, V.P. Val'chuk, *Chemical Physics Letters* **233** (1995) 63.
- [7] S. Pei, H.M. Cheng, *Carbon* **50** (2012) 3210.
- [8] K.S. Novoselov, A.K. Geim, S.V. Morozov, D. Jiang, M.I. Katsnelson, I.V. Grigorieva, S.V. Dubonos, A.A. Firsov, *Nature* **438** (2005) 197.
- [9] Y. Sun, Q. Wu, G. Shi, Q. Zhang, *Energy and Environmental Science* **4** (2011) 1113.
- [10] D.R. Dreyer, S. Park, C.W. Bielawski, R.S. Ruoff, *Chemical Society Reviews* **39** (2010) 228.
- [11] W. Gao, L.B. Alemany, L. Ci, P.M. Ajayan, *Nature Chemistry* **1** (2009) 403.
- [12] S. Park, R.S. Ruoff, *Nature Nanotechnology* **4** (2009) 217.
- [13] G. Eda, M. Chhowalla, *Advanced Materials* **22** (2010) 2392.
- [14] Y. Xu, K. Sheng, C. Li, G. Shi, *ACS Nano* **4** (2010) 4324.
- [15] J.R. Potts, D.R. Dreyer, C.W. Bielawski, R.S. Ruoff, *Polymer* **52** (2011) 5.
- [16] X. Li, W. Cai, J. An, S. Kim, J. Nah, D. Yang, R. Piner, A. Velamakanni, I. Jung, E. Tutuc, S.K. Banerjee, L. Colombo, R.S. Ruoff, *Science* **324** (2009) 1312.
- [17] Y. Hernandez, V. Nicolosi, M. Lotya, F.M. Blighe, Z. Sun, S. De, I.T. McGovern, B. Holland, M. Byrne, Y.K. Gun'Ko, J.J. Boland, P. Niraj, G. Duesberg, S. Krishnamurthy, R. Goodhue, J. Hutchison, V. Scardaci, A.C. Ferrari, J.N. Coleman, *Nature Nanotechnology* **3** (2008) 563.
- [18] K.R. Paton, E. Varrla, C. Backes, R. J. Smith, U. Khan, A. O'Neill, C. Boland, M. Lotya, O.M. Istrate, P. King, T. Higgins, S. Barwich, P. May, P. Puczkarski, I. Ahmed, M. Moebius, H. Pettersson, E. Long, J. Coelho, S.E. O'Brien, E.K. McGuire, B.M. Sanchez, G.S. Duesberg, N. McEvoy, T.J. Pennycook, C. Downing, A. Crossley, V. Nicolosi, J.N. Coleman, *Nature Materials* **13** (2014) 624.
- [19] F. Bonaccorso, Z. Sun, T. Hasan, A.C. Ferrari, *Nature photonics* **4** (2010) 611.
- [20] K.S. Kim, Y. Zhao, H. Jang, S.Y. Lee, J.M. Kim, K.S. Kim, J.H. Ahn, P. Kim, J.Y. Choi, B.H. Hong, *Nature* **457** (2009) 706.

- [21] Y. Hernandez, V. Nicolosi, M. Lotya, F.M. Blighe, Z. Sun, S. De, I.T. McGovern, B. Holland, M. Byrne, Y.K. Gun'Ko, J.H. Boland, P. Niraj, G. Duesberg, S. Krishnamurthy, R. Goodhue, J. Hutchison, V. Scardaci, A.C. Ferrari, J.N. Coleman, *Nature Nanotechnology* **3** (2008) 563.
- [22] Y. Xu, H. Bai, G. Lu, C. Li, G. Shi, *Journal of the American Chemical Society* **130** (2008) 5856.
- [23] C. Gómez-Navarro, M. Burghard, K. Kern, *Nano Letters* **8** (2008) 2045.
- [24] W. Yang, K.R. Ratinac, S.P. Ringer, P. Thordarson, J.J. Gooding, F. Braet, *Angewandte Chemie International Edition* **49** (2010) 2114.
- [25] H. Chen, M.B. Müller, K.J. Gilmore, G.G. Wallace, D. Li, *Advanced Materials* **20** (2008) 3557.
- [26] Z. Liu, J.T. Robinson, X. Sun, H. Dai, *Journal of the American Chemical Society* **130** (2008) 10876.
- [27] S.K. Krishnan, E. Singh, P. Singh, M. Meyyappan, H.S. Nalwa, *RSC Advances* **9** (2019) 8778.
- [28] A.C. Ferrari, J.C. Meyer, V. Scardaci, C. Casiraghi, M. Lazzeri, F. Mauri, S. Piscanec, D. Jiang, K.S. Novoselov, S. Roth, A.K. Geim, *Phys. Rev. Lett.* **97** (2006) 187401.
- [29] K. Tian, Z. Su, H. Wang, X. Tian, W. Huang, C. Xiao, *Composites: Part A: Applied Science and Manufacturing* **94** (2017) 41.
- [30] A.B.D. Nandiyanto, R. Oktiani, R. Ragadhita, *Indonesian Journal of Science & Technology* **4** (2019) 97.
- [31] B.C. Smith, *Spectroscopy* **32** (2017) 19
- [32] T. Peng, H. Sun, T. Peng, B. Liu, X. Zhao, *Nanomaterials* **7** (2017) 292.
- [33] Y.N. Patel, M.P. Patel, *Journal of Macromolecular Science, Part A: Pure and Applied Chemistry* **49** (2012) 490.
- [34] S. Mahalingam, M. Durai, C. Sengottaiyan, Y.H. Ahn, *Journal of Nanoscience and Nanotechnology* **21** (2021) 3183.
- [35] F. Zanella, K.Z. Nobrega, C.A. Dartora, *Physica E: Low-dimensional Systems and Nanostructures* **84** (2016) 16.
- [36] M.S. Jimenez, C.A. Dartora, *Physica E: Low-dimensional Systems and Nanostructures* **59** (2014) 1.